Long-Term Drainage Reduces CO2 Uptake and CH4 Emissions in a Siberian Permafrost Ecosystem

Kittler, Fanny

2017-12

Kittler , F , Heimann , M , Kolle , O , Zimov , N , Zimov , S & Gockede , M 2017 , ' Long-Term Drainage Reduces CO2 Uptake and CH4 Emissions in a Siberian Permafrost Ecosystem ' , Global Biogeochemical Cycles , vol. 31 , no. 12 , pp. 1704-1717 . https://doi.org/10.1002/2017GB005774

http://hdl.handle.net/10138/308103
https://doi.org/10.1002/2017GB005774

AGU PUBLICATIONS

Global Biogeochemical Cycles

RESEARCH ARTICLE
10.1002/2017GB005774

Key Points:
- Systematic shifts in tundra ecosystem carbon cycle patterns triggered by drained soils with decreased CO_2 uptake and CH_4 emissions
- Year-round measurements emphasize the importance of the non-growing season—in particular the freeze-in period—to the annual budget
- Temperature variability during the late growing season was identified as the primary control of the interannual flux variability

Supporting Information:
- Supporting Information S1
- Figure S1

Correspondence to:
F. Kittler,
fkittler@bgc-jena.mpg.de

Citation:
Kittler, F., Heimann, M., Kolle, O., Zimov, N., Zimov, S., & Göckede, M. (2017). Long-term drainage reduces CO_2 uptake and CH_4 emissions in a Siberian permafrost ecosystem. *Global Biogeochemical Cycles*, *31*, 1704–1717. https://doi.org/10.1002/2017GB005774

Received 3 AUG 2017
Accepted 3 DEC 2017
Accepted article online 12 DEC 2017
Published online 20 DEC 2017

Long-Term Drainage Reduces CO_2 Uptake and CH_4 Emissions in a Siberian Permafrost Ecosystem

Fanny Kittler[1], Martin Heimann[1,2], Olaf Kolle[1], Nikita Zimov[3], Sergei Zimov[3], and Mathias Göckede[1]

[1]Max Planck Institute for Biogeochemistry, Jena, Germany, [2]Division of Atmospheric Sciences, University of Helsinki, Helsinki, Finland, [3]North-East Science Station, Pacific Institute for Geography, Far-Eastern Branch of Russian Academy of Science, Cherskii, Russia

Abstract Permafrost landscapes in northern high latitudes with their massive organic carbon stocks are an important, poorly known, component of the global carbon cycle. However, in light of future Arctic warming, the sustainability of these carbon pools is uncertain. To a large part, this is due to a limited understanding of the carbon cycle processes because of sparse observations in Arctic permafrost ecosystems. Here we present an eddy covariance data set covering more than 3 years of continuous CO_2 and CH_4 flux observations within a moist tussock tundra ecosystem near Chersky in north-eastern Siberia. Through parallel observations of a disturbed (drained) area and a control area nearby, we aim to evaluate the long-term effects of a persistently lowered water table on the net vertical carbon exchange budgets and the dominating biogeochemical mechanisms. Persistently drier soils trigger systematic shifts in the tundra ecosystem carbon cycle patterns. Both, uptake rates of CO_2 and emissions of CH_4 decreased. Year-round measurements emphasize the importance of the non-growing season—in particular the "zero-curtain" period in the fall—to the annual budget. Approximately 60% of the CO_2 uptake in the growing season is lost during the cold seasons, while CH_4 emissions during the non-growing season account for 30% of the annual budget. Year-to-year variability in temperature conditions during the late growing season was identified as the primary control of the interannual variability observed in the CO_2 and CH_4 fluxes.

1. Introduction

Arctic temperatures rise faster than the global average (Overland et al., 2014; Serreze et al., 2009), and climate models also predict a strong high-latitude warming for the future (IPCC, 2013). Because Arctic ecosystems are highly susceptible to shifts in environmental conditions, changes in the temperature regime will also affect the local carbon cycle processes (McGuire et al., 2009; Schuur et al., 2015). During the last glacial cycle in the northern circumpolar permafrost region, an estimated 1,035 Pg of organic carbon (Hugelius et al., 2014) has accumulated within the soil layer down to 3 m below surface because of slowed decomposition under low temperatures and anoxic conditions. The sustainability of this carbon pool is strongly dependent on future climate conditions (Kaufman et al., 2009; Kirschbaum, 1995; Serreze et al., 2000).

Under scenarios of moderate climate warming, up to 30% of Arctic lowland landscapes (Jorgenson, Shur, & Pullman, 2006) could be affected by altered geomorphology. In turn, hydrologic conditions may also systematically change, e.g., through the process of ice wedge degradation (Liljedahl et al., 2016). Manipulation experiments focusing on changes in spatiotemporal patterns of soil water availability can give valuable insight into the complex potential shifts in ecosystem characteristics associated with persistently drier conditions. These include changes in and interactions between soil thermal regime, vegetation and microbial community composition, and snow cover regimes, all of which can trigger systematic shifts in carbon cycle processes. Only a few such field manipulations have been conducted in the Arctic thus far. These were performed on a small spatial (Oechel et al., 1998; Strack, Kellner, & Waddington, 2006) or temporal scale (Merbold et al., 2009). A large-scale water table manipulation experiment in Alaska revealed an increase in the CO_2 loss (Zona et al., 2012) and a decrease in CH_4 emissions (Sturtevant et al., 2012; Zona et al., 2009) under drained conditions. Similar trends regarding the systematic influence of a drainage disturbance on the summertime budgets of carbon (Kittler et al., 2016; Kwon et al., 2017, 2016) and energy fluxes (Göckede et al., 2016) have been reported for the experiment site close to Chersky in NE Siberia that is also the subject of the present study.

Because of the remoteness of large parts of the Arctic, these ecosystems are difficult to access, and continuous monitoring programs are impeded by logistical challenges. Moreover, extreme climate conditions pose special demands on both instrumentation and power sources (Goodrich et al., 2016), thereby resulting in a comparatively sparse data coverage of carbon flux measurements for the Arctic (Oechel et al., 2014; Zona et al., 2016). Studies focusing on CO_2 fluxes in Arctic regions with underlying permafrost reveal a pronounced variability regarding the direction and magnitude of annual flux budgets. Results range from net sources (Euskirchen et al., 2012, 2016; Oechel et al., 2014; Zimov et al., 1996) to CO_2-neutral (Lüers et al., 2014) to net sinks (Aurela et al., 2007; Aurela, Laurila, & Tuovinen, 2004; Kutzbach, Wille, & Pfeiffer, 2007; Lund et al., 2012; Pirk et al., 2017). Modeling results are also spread over a wide range (Belshe, Schuur, & Bolker, 2013; McGuire et al., 2012). Initial year-round eddy covariance measurements of CO_2 fluxes from continuous permafrost (Oechel et al., 2014) demonstrated that the non-growing season significantly contributes to the annual budget. Studies focusing on multiyear observations identified climatic conditions (Arneth et al., 2002; Merbold et al., 2009) with a specific focus on temperature and temperature-related variables such as snow-melt timing (Aurela et al., 2004; Philipp et al., 2016), growing degree days (Euskirchen et al., 2012), and maximum thaw depth (Lund et al., 2012) as the most important controlling factors for interannual variability of CO_2 fluxes.

While Arctic ecosystems usually act as sustained sources of CH_4, flux magnitudes are associated with large uncertainties (Christensen, 2014), and data coverage is even sparser than for CO_2. Published annual CH_4 emissions range between 7 gC m^{-2} (Tagesson et al., 2012) and 13 gC m^{-2} (Rinne et al., 2007). Based on recent observations, the cold season accounts for up to 50% of the annual CH_4 budget. Large emissions occur during the "zero-curtain" period, which represents the refreezing period of the active layer during fall (Zona et al., 2016). While some studies observed burst events of CH_4 fluxes during the refreezing of the active layer (Mastepanov et al., 2008; Tagesson et al., 2012), others report continuous CH_4 efflux during the fall period (Sturtevant et al., 2012; Wille et al., 2008). Environmental controls such as soil temperature and near-surface atmospheric turbulence (Wille et al., 2008), soil moisture (Sturtevant et al., 2012), and vegetation (Turetsky et al., 2014) can influence the interannual variability of CH_4 fluxes (Emmerton et al., 2014; Mastepanov et al., 2013; Moore et al., 2011).

In summary, the understanding of Arctic carbon flux budgets and therefore also our ability to predict the sustainability of Arctic carbon pools in light of climate change is significantly hampered by the limited database of year-round observations. Particularly for CH_4 fluxes, only few continuous flux time series for the non-growing season have been published. For CO_2, most observations during the winter seasons have been compromised by considerable data gaps during the harsh polar winter conditions.

To improve this situation and advance the understanding of carbon exchange between surface and atmosphere in Arctic permafrost ecosystems, we established a monitoring program near Chersky in northeastern Siberia, which has been operated continuously since mid-July 2013. In this study, we present the seasonal flux patterns and annual budgets of CO_2 and CH_4 of two eddy covariance towers running in parallel over a disturbed tundra ecosystem (i.e., a drainage ditch ring installed in 2004 that mimics the degradation of ice rich permafrost) and a control tundra ecosystem representing natural conditions, respectively. Our analyses compare data sets covering over 3 years of continuous flux measurements in combination with ancillary data to analyze the drivers of the interannual variability.

2. Material and Methods

2.1. Site Description

The research site, which is located in a floodplain of the Kolyma river near Chersky (68.75°N, 161.33°E), NE Russia, consists of a wet tussock tundra dominated by tussock-forming C*arex appendiculata* and *lugens* and *Eriophorum angustifolium* (Kwon et al., 2016). An organic peat layer (0.15–0.20 m) overlays alluvial mineral soils (silty clay) with some organic material also present in deeper layers following cryoturbation (Corradi et al., 2005; Kwon et al., 2016; Merbold et al., 2009). For 2014–2016, mean annual air temperature was −10.2°C (daily means ranging between −49.8°C in January 2014 and 24.6°C in July 2015). A total annual precipitation of 160 mm was observed during this period. This is about 20% lower than the average of 197 mm observed during the period of 1960–2009. During the transition period in late spring (May/June), site hydrology is strongly influenced by flooding as a result of snowmelt and rising water levels in the nearby river. This resulted in standing water on the site (up to 0.5 m above ground surface) in most years. Afterward, the water table decreased gradually within days to weeks depending on fine-scale microsite conditions. The seasonal development of the vegetation is usually delayed in wet compared to dry areas, where snowmelt is followed by rapid greening. Vegetation height reached ~0.7 m at the end of the growing season. Snow cover thickness was on average 0.8 m and peaked around April with maximum snow depth reaching over 1 m in 2015.

Since fall 2004, a circular drainage ditch with a diameter of ~200 m connected to the nearby river has been modifying the local hydrology and soil moisture condition. The circular drainage ditch resulted in a locally reduced water table (up to 0.3 m in summer; Kwon et al., 2016; Merbold et al., 2009). More detailed information on site conditions can be found under undisturbed conditions (Corradi et al., 2005), immediate drainage effects (Merbold et al., 2009), and long-term drainage effects on ecosystem structure and energy fluxes (Göckede et al., 2016) as well as on carbon fluxes (Kittler et al., 2016; Kwon et al., 2017, 2016).

2.2. Instrument Setup and Data Processing

Two identical observation systems were installed: one within the drainage area (hereafter referred to as drained site) and a second representing natural condition (hereafter referred to as control site). Ecosystem-scale fluxes were monitored with eddy covariance systems at a site elevation of 6 m above sea level. One tower (drained, 68.61°N and 161.34°E) was placed within the drainage. The footprint primarily covered the area affected by the reduced water table. The second tower (control, 68.62°N and 161.35°E) was installed ~600 m away representing natural conditions unaffected by the disturbance. At both towers, continuous data acquisition started in July 2013 (13th and 16th for the drained and control tower, respectively).

Towers were equipped with a heated sonic anemometer (uSonic-3 Scientific, 5 W heating, Metek GmbH, Elmshorn, DE) on top (at heights of 4.9 m and 5.1 m for drained and control tower, respectively) as well as a gas analyzing system. Measurements started with open-path sensors (LI-7500, LI-COR Biosciences Inc., NE, USA) for CO_2 and H_2O flux densities placed next to the sonic with a sensor separation of 0.38 m at both towers. In April 2014, closed-path gas analyzers (FGGA, Los Gatos Research Inc., CA, USA) for monitoring CO_2, H_2O, and CH_4 mixing ratios were added along with an inlet placed next to the sonic anemometer (vertical sensor separation: 0.30 m), a sampling line (heated and insulated Eaton Synflex decabon with 6.2 mm inner diameter and a length of 16 m and 13 m for drained and control tower, respectively), and an external vacuum pump (membrane pump, N940, KNF, 13 L min^{-1} under ambient pressure). Both gas analyzing systems have been running in parallel at the drained tower since April 2014, while the open-path analyzer at the control tower was disassembled in July 2014. The final time series for CO_2 fluxes used in this study are a product of merged data from open-path (July 2013 to April 2014) and closed-path (since April 2014) gas analyzers.

High-frequency eddy covariance data were collected with 20 Hz and acquired through the software package EDDYMEAS (Kolle & Rebmann, 2007) on a local computer at the field site. Flux calculation of eddy covariance data was based on the software tool TK3 (Mauder & Foken, 2015), which implemented all standardized methods (Fratini & Mauder, 2014) to process and correct fluxes including 2-D coordinate rotation of the wind field, cross-wind correction (Liu, Peters, & Foken, 2001), and correction for losses in the high-frequency range (Moore, 1986). Closed-path data were converted from wet mole fraction to mixing ratios before the flux processing. For open-path data, the density-flux WPL correction (Webb et al., 1980) and the self-heating correction were applied. Details of the self-heating correction approach are described in Kittler et al. (2017). The self-heating correction approach follows Järvi et al. (2009) based on Burba et al. (2006) by comparing CO_2 flux measurements between open- and closed-path gas analyzers. The instrument surface temperature T_s was estimated from the air temperature T_a based on polynomial fit from a field experiment: $T_s = 0.0025\ T_a^2 + 0.9\ T_a + 2.07$ (Burba et al., 2006). Since the open-path analyzer is mounted in an inclined position, only a fraction of the full correction is required that is represented by a scaling factor, which was optimized separately for daytime and nighttime conditions.

The post-processing quality control and flagging system scheme was based on stationarity and well-developed turbulence proposed by Foken and Wichura (1996) followed by additional tests applied to flag implausible data points in the resulting flux time series. Tests included absolute limits for flux data ($-15\ \mu mol\ m^{-2}\ s^{-1} < CO_2$ flux $< 5\ \mu mol\ m^{-2}\ s^{-1}$and $-0.05\ \mu mol\ m^{-2}\ s^{-1} < CH_4$ flux

Table 1
Mean Data Coverage in Percentage of CH_4 Fluxes Per Season and Site, Excluding Data From End-October 2015 to Mid-July 2016 for Both Towers When the Closed-Path Analyzer at the Control Site Was Not Active

Season	Drained (%)	Control (%)
Spring	72	76
Growing	80	86
Fall	77	85
Winter	70	67

< 0.3 μmol m^{-2} s^{-1}), the open-path gas analyzing system status information (gain control maximum >75), overall errors in the log file recorded by the sonic anemometer, a comparison of the absolute concentrations of CO_2 for the two towers for specific wind directions to detect potential contamination by the exhaust plume of the generator (distance ~300 m; based on a more than 5% difference criterion), an air temperature threshold (< −40°C, which is the lowest possible operating temperature for the sonic anemometer), a flag for sonic anemometer heating, and a flag for spikes for the CH_4 flux. Quality flags were combined, and data covering quality flags 1–6 (Foken et al., 2005, 2012) were used for a reliable and robust gap filling procedure.

Data coverage of CO_2 fluxes for the closed-path system ranged between 60 and 80% during the growing season and between 50 and 60% during winter season. For the open-path systems, data coverage was lower because of additional gaps caused by unfavorable weather conditions affecting measurements (e.g., rain and condensation). Data coverage of CH_4 fluxes is reported in Table 1. Longer gaps were caused by flooding events, during which the entire system needed to be shut down to avoid damage, or a laser offset in the closed-path gas analyzer at Tower 1 in 2015. No data for CO_2 and CH_4 was available at the control site from end-October and mid-December 2015, respectively, until mid-July 2016.

Gap filling and flux partitioning for CO_2 fluxes were implemented through the R package REddyProc (https://r-forge.r-project.org/projects/reddyproc/; Reichstein et al., 2005). Gap filling was based on the condition variable season, global radiation, and vapor pressure deficit. For the flux partitioning, the definition of nighttime conditions was set to a radiation threshold (20 W m^{-2}; e.g., Parmentier et al., 2011, Runkle et al., 2013). To address the temperature dependence of ecosystem respiration, air temperature was used. The gap filling procedure for CH_4 fluxes is based on means of a 10 day moving window (centered around the gap). For annual budgets, mean annual cycles for each tower and gas species were used to fill long gaps.

A suite of environmental variables was collected along with the high-frequency eddy covariance data at both towers simultaneously. An overview can be found in Kittler et al. (2016). Meteorological data were collected at 10 s intervals and stored on a data logger (CR3000, Campbell Scientific Inc., UT, USA) as averages over 10 min periods. After the post-processing quality control scheme (including tests for failure of the power supply, ranges and consistency limits, missing variability, spikes, and sensor malfunction), the final data set was averaged to 30 min.

2.3. Seasonality Analysis

The beginning of the spring season was defined by a net radiation threshold (>0 W m^{-2} for four consecutive days) according to Oechel et al. (2014). The growing season was defined by a combination of daily mean air temperature (>4°C for four consecutive days as starting point) and fractional snow cover (>50% as endpoint, determined by Moderate Resolution Imaging Spectroradiometer (MODIS) normalized difference vegetation index data with both daily and 16 day temporal resolutions). The end of fall was determined by the end of the zero-curtain period (Zona et al., 2016) by using 0.32 m soil temperature data at the drained site. The interannual variability of the starting dates for the seasonal deviations is shown in Table 2.

Table 2
Interannual Variability in Starting Dates Per Season, With Dates Given as Day of Year (DOY)

Start of season	2013	2014	2015	2016
Spring	-	119	108	102
Growing season	149	153	151	138
Fall	273	281	264	269
Winter	293	338	330	362

3. Results

3.1. Seasonal Contribution

The growing season dominates the annual cycle with both the highest flux rates and cumulative budgets (Figures 1 and 2). Net CO_2 uptake by the ecosystem (negative flux rates) only occurs around peak growing season when vegetation uptake outweighs respirational losses. During the remaining parts of the year, net CO_2 emissions (positive flux rates) dominate (Figure 1a). The highest CH_4 emission rates during the growing season (Figure 1b) are triggered by increased production rates

10.1002/2017GB005774

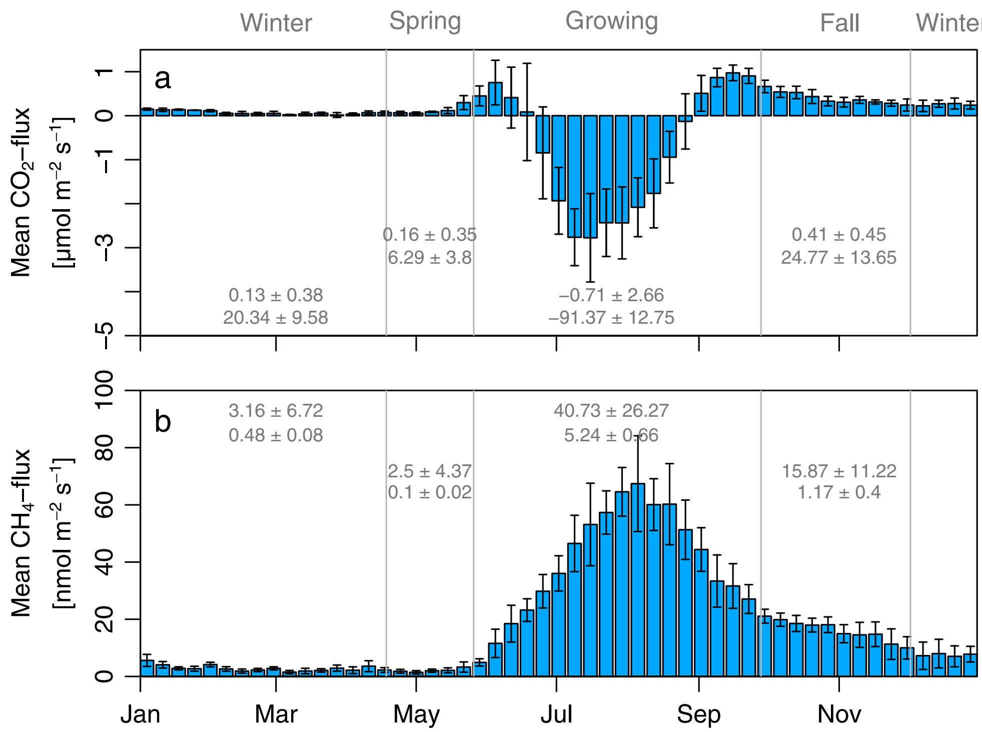

Figure 1. Averaged annual cycle as weekly means (colored bars) and standard deviation (error bars) for (a) CO_2 and (b) CH_4 at the control site. The number (both as mean ± SD) represents seasonal mean flux rates (top number) and cumulative flux budgets per season (bottom number in gC m^{-2}).

linked to high soil temperatures and efficient plant-mediated transport rates resulting from a higher abundance of aerenchymatous plants.

In fall, during the zero-curtain period, flux rates remain at comparably high levels with substantial net emissions for both CO_2 and CH_4 (Figure 1). Accordingly, this period significantly contributes to the net annual flux budgets, emitting ~27% of the growing season CO_2 uptake and adding ~23% to the growing season budget of CH_4. Emissions continue into the winter (Figure 1), but average flux rates are minor compared to fall. Nevertheless, because of the length of this season (i.e., on average 144 days), when accumulated these small winter season emissions make a considerable contribution to the annual budget. In total, all non-growing seasons combined systematically affect the annual budget, emitting 56% of the growing season CO_2 uptake and adding 33% to the growing season budget of CH_4 emissions.

3.2. Drainage Impact on Annual Carbon Budgets

Our data set, which includes interpolated sections, covers continuous eddy covariance observations with 4 years of CO_2 fluxes and 3 years of CH_4 fluxes (Figure 2). Cumulative budgets demonstrate that in each data year, drainage systematically altered the CO_2 fluxes of this Arctic floodplain ecosystem (Figure 2a and Table 3). The mean reduction of the annual sink strength in CO_2 following the drainage disturbance is 47.5 ± 11.1 gC m^{-2}. Annual differences range from 37.8 gC m^{-2} in 2014 to 62.0 gC m^{-2} in 2015. Partitioning of the net CO_2 fluxes into photosynthetic uptake (gross primary production (GPP)) and respiration losses (Reco) during the growing season (see Figure S1 in the supporting information) reveal that moderate increases in GPP following drainage are outweighed by higher respiration losses.

The CH_4 flux rates at the control site continually exceeded emissions at the drained site representing drier and therefore more aerobic conditions (Figure 2b and Table 3). The mean absolute annual budget difference between drained and control ecosystems was 3.3 ± 0.5 gC m^{-2}. The maximum was 3.7 gC m^{-2} in 2016.

Focusing on the two data years (2014 and 2015) in which large data gaps are absent at both sites, systematic differences between drained and control site have been determined Figure 3). For CO_2, the net emissions at

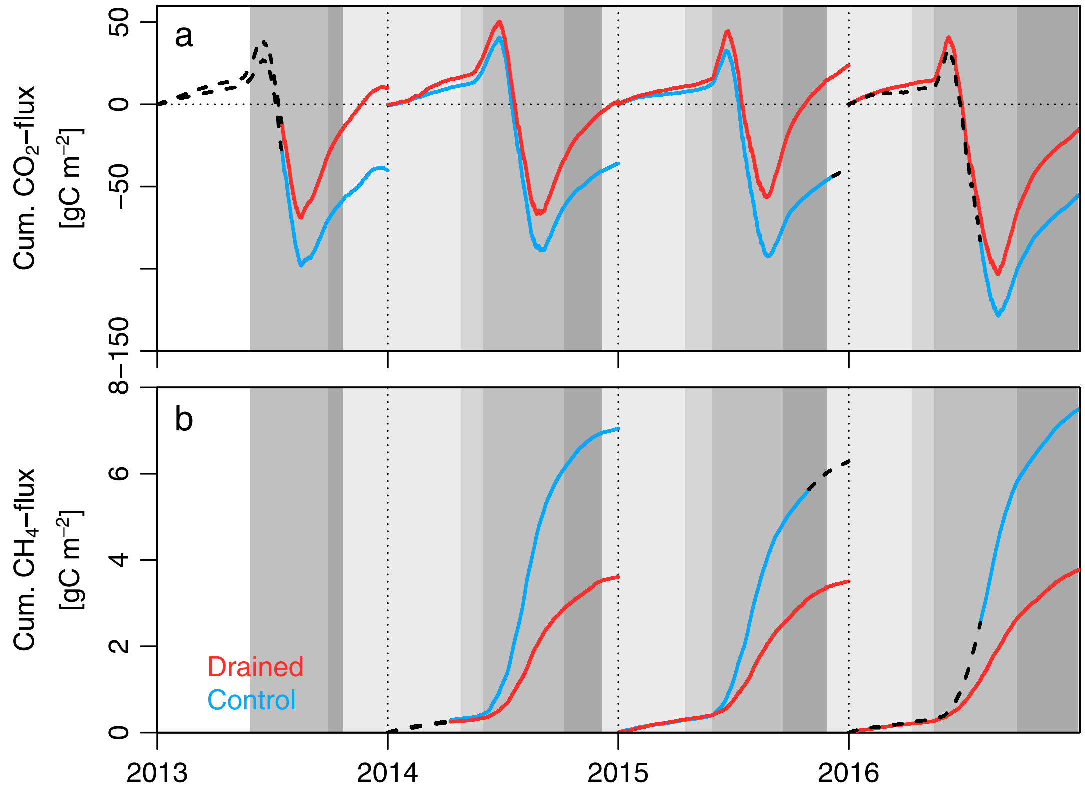

Figure 2. The cumulative budget for (a) CO_2 and (b) CH_4 from drained (red) and control (blue) ecosystems was calculated separately for each data year. Long gaps (black dashed lines) were filled using mean annual cycle trends. The background shading indicates the seasons from winter (light gray) to fall (dark gray).

the drained site (Table 3) and the strong negative budget at the control site (Table 3) add up to a net drainage impact of 50 gC m^{-2} (Figure 3). Accordingly, drainage turns this tundra site into a moderately higher source for atmospheric CO_2. In contrast, CH_4 emissions at the drained site are systematically lower than those at the control site (Table 3), thereby yielding a net reduction in the source strength for atmospheric CH_4 of −3 gC m^{-2} (Figure 3) following drainage. At both sites, the shifts in the total carbon mass budget are dominated by the CO_2 fluxes. The drainage thus triggers a net loss of carbon (47 gC m^{-2}; Figure 3) to the atmosphere.

We employed global warming potential metrics to convert CH_4 fluxes into $CO_{2,\ eq.}$ using a conversion factor of 34 for a 100 year integration time frame. Based on these metrics, the drainage disturbance increases the source of $CO_{2,\ eq.}$ to the atmosphere by 12 gC m^{-2} (Figure 3). The pronounced additional source of CO_2 as resulting from the drainage is largely balanced by reductions in CH_4 emissions. However, the changes in the CO_2 budget still dominate the $CO_{2,\ eq.}$ budget.

Table 3
CO_2 and CH_4 Annual Budgets Focusing on the Whole Observation Period (2013–2016) and on the Two Data Years (2014 and 2015), in Which Large Data Gaps Are Absent

Time period	Site	CO_2 (gC m^{-2})	CH_4 (gC m^{-2})
2013–2016	Drained	5.2 ± 16.1	3.6 ± 0.1
	Control	−42.3 ± 8.5	7.0 ± 0.6
2014–2015	Drained	12.9 ± 15.4	3.6 ± 0.1
	Control	−37.1 ± 1.7	6.7 ± 0.5

Note. All values are given as mean ± standard deviation.

3.3. Interannual Variability and Controlling Factors

By assigning start and end dates to specific seasons based on *in situ* and remote sensing information on environments conditions and calculating the cumulative budgets per season, we attributed variabilities in net annual flux budgets to specific parts of the year (Figure 4). Our results demonstrate that flux rates in spring (Figures 4b and 4g), fall (Figures 4d and 4i), and winter (Figures 4a, 4e, 4f, and 4j) follow a uniform seasonal pattern in all data years, thereby resulting in similar seasonal CO_2 and CH_4 budgets, which are independent of prevailing environmental conditions such as snow depth or mean season temperatures. Year-to-year variability in both CO_2 and CH_4 data is therefore almost exclusively caused by pronounced shifts in carbon exchange

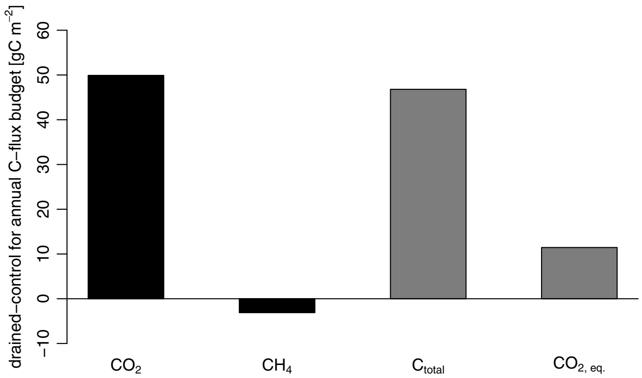

Figure 3. Carbon dioxide, methane, total carbon (C_{total} as sum of CO_2 and CH_4), and $CO_{2,\ eq.}$ by accounting for the global warming potential budget for CH4 under a 100 year time horizon with inclusion of climate–carbon feedbacks (IPCC, 2013) averaged annually for the data years 2014 and 2015 as differences between drained and control site.

processes during the growing season, during which major differences in both absolute flux rates and temporal patterns have been observed (Figures 4c and 4h). This variability is not driven by the length of the season, which ranges between 113 days in 2015 and 131 days in 2016.

During the growing season, a pronounced year-to-year variability is observed for CO_2 at both sites (Figure 4c). In contrast, CH_4 emission rates at the drained site are uniform over all data years, and variability can only be observed at the control site (Figure 4h). For both CO_2 and CH_4 in the first part of the growing season (first 60 days), flux time series are rather uniform in all data years (Figures 4c and 4h).

By linking the cumulative CO_2 budgets during both parts of the growing season to mean air temperatures in the respective periods, contrasting dependencies are found (Figure 5). In the first part of the growing season, in which no variability in CO_2 exchange was observed between data years, our findings show no correlation at all with the interannual variability in mean air temperatures (Figure 5a). During the second part of the growing season, there is a direct linear relationship between mean air temperature and the cumulative CO_2 budget (Figure 5b).

Methane emission rates at the drained site are uniform within all data years. Only data from the control site with pronounced interannual variability was used for the analysis. Furthermore, the data year 2016 was excluded because data were only available for the second part of the growing season (Figure 2b). Methane emissions at the control site display similar characteristics as observed for the CO_2 fluxes; i.e., we found uniform flux rates during the first part of the growing season (up to 60 days with ~2 gC m^{-2}; Figure 4c) and a pronounced year-to-year variability during the second part of the growing season (day 61 to end of the season; Figure 4c). Emission rates during the second part of the growing season are higher in 2014 (3.3 gC m^{-2}) compared to 2015 (2.2 gC m^{-2}). Differences were mostly triggered by soil temperature conditions (Figure 6), while soil moisture measurements indicate uniform conditions close to saturation in

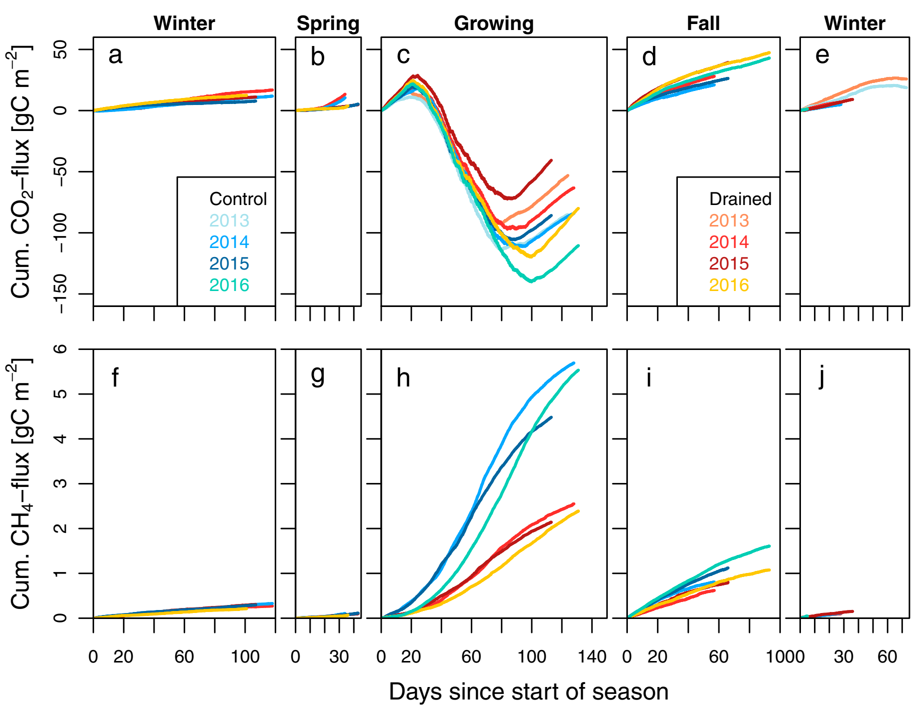

Figure 4. Cumulative (a–e) CO_2 and (f–j) CH_4 budgets. Time series were separated into the four different seasons (see section 2.2), and budgets were reset to zero at the beginning of each season.

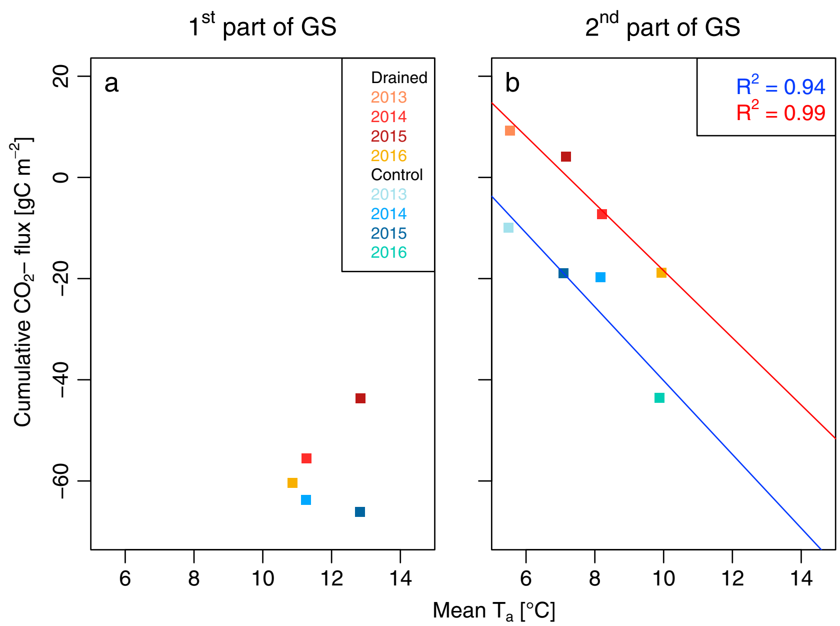

Figure 5. Cumulative CO_2 flux in relation to mean air temperature measured at 2 m height separated into first part of the growing season (up to 60 days) and second part of growing season (day 61 to end of season). The lines are based on the standard least squares regression. Since measurements started mid-July 2013, data from both towers for the first part of the growing season 2013 are not shown. Also data from the control site for the first part of the growing season 2016 are excluded due to a long data gap.

both data years. In the growing season 2014, a tendency toward higher than average soil temperatures was observed, leading to increased CH_4 emissions. In contrast, during the second part of the growing season in 2015, soil temperatures below the mean resulted in reduced CH_4 emissions.

4. Discussion

4.1. Seasonal Contribution

The mean average annual CO_2 uptake of 42 gC m^{-2} are within the range of the reported net uptake results for Arctic permafrost ecosystems (Aurela et al., 2004, 2007; Kutzbach et al., 2007). However, our findings differ

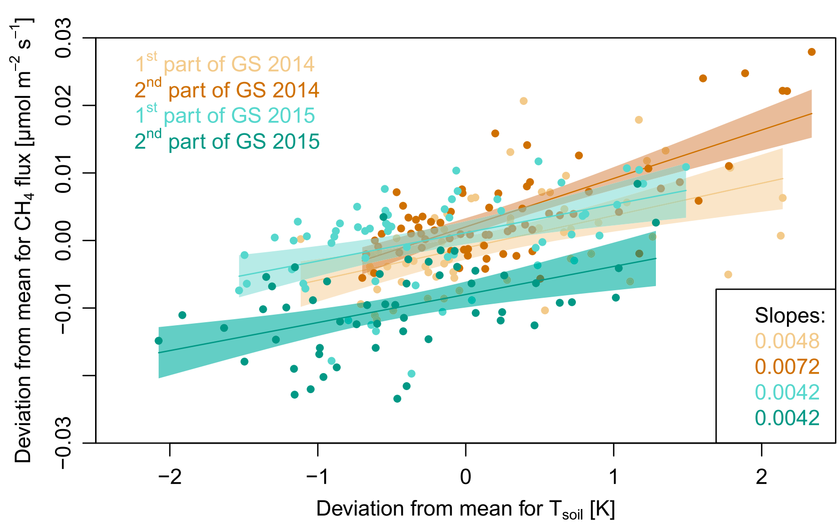

Figure 6. Deviations from mean annual cycle with daily means for CH_4 fluxes and soil temperatures (T_{soil}) in 0.08 m depth. Data are restricted to the growing season and are separated into two parts following Figure 5. The lines are based on the standard least squares regression with confidence intervals as shaded area.

systematically from the observations by other studies, i.e., 14 gC m^{-2} for a moist acidic tundra in Alaska (Oechel et al., 2014) and -19 gC m^{-2} for a polygonal tundra in northern Siberia (Kutzbach et al., 2007), which cover environmental conditions (e.g., mean annual air temperature or ecosystem type) similar to those at our site near Chersky. Following the growing season that typically features a pronounced CO_2 uptake (Euskirchen et al., 2016) peaking around July (Jammet et al., 2017), the fall is associated with major CO_2 losses (Kwon et al., 2016; Laurila et al., 2001; Mikhailov et al., 2013) that result in nonnegligible contributions of the fall season to the annual budget, which is in agreement with previous studies (Christiansen, Schmidt, & Michelsen, 2012; Kutzbach et al., 2007; Lüers et al., 2014; Oechel et al., 2014). Our findings confirm reports of cold season emissions contributing more than 50% of the annual budget (including spring; Kutzbach et al., 2007). For some studies, fall and winter emission even outbalanced the growing season uptake (Lüers et al., 2014; Oechel et al., 2014). Differences in the winter season flux budgets are largely attributed to interannual variability in the cold season soil temperatures, which, in turn, are strongly controlled by snow cover dynamics (Morgner et al., 2010; Yu et al., 2016) and latent heat effects associated with soil moisture levels. Sustained warmer conditions in soils during winter commonly lead to higher CO_2 emission rates (Webb et al., 2016).

Mean annual CH_4 emissions of 7 gC m^{-2} are lower than previously reported year-round rates within northern wetland ecosystems. For example, much higher mean emission rates during all seasons for a thawed fen of a subarctic peatland (Jammet et al., 2017) and about twice the mean annual CH_4 budget from a boreal fen (Rinne et al., 2007) were observed. On the other hand, winter contributions amounting to approximately 7% of the total annual CH_4 emissions are comparable to other studies (Rinne et al., 2007). Remaining differences are mainly associated with lower year-round temperatures at our site, which reduce microbial activity (Lloyd & Taylor, 1994). Annual CH_4 budgets are comparable to similar ecosystem types—even while differences in many other aspects (e.g., measurement technique, observation period, and active layer thickness) are present (Tagesson et al., 2012). Regarding the analysis of seasonal contributions, in agreement with previous studies (Jammet et al., 2017), growing season CH_4 emissions peak around August, but substantial CH_4 emissions were also observed during fall (Mastepanov et al., 2013; Wille et al., 2008). However, our data sets do not include any significant CH_4 outburst events during the freezeup period (Mastepanov et al., 2008; Tagesson et al., 2012). Adding over 20% to the growing season emissions, the zero-curtain period in fall represents the second most important season for CH_4 emissions (Sturtevant et al., 2012). In total, cold season emissions account for approximately 30% of the annual CH_4 budget, which is a substantial fraction but less than reported by Zona et al. (2016), who found a strong dependency of emission rates on the duration and depth of the unfrozen soil.

In summary, our data sets emphasize the elevated importance of high-quality year-round observations for producing reliable carbon flux budgets for Arctic ecosystems. Neglecting fluxes outside the growing season would lead to significant biases in year-round flux budgets (Oechel, Vourlitis, & Hastings, 1997), and in case of our study site would lead to an overestimation of the CO_2 sink by approximately 60%, and an underestimation of the CH_4 source by approximately 30% at our observation sites near Chersky. Accordingly, land-surface modeling schemes that are exclusively calibrated on growing season data sets for permafrost ecosystems will produce a biased representation of the current role of the Arctic in the global carbon budget. Future projections on permafrost carbon-climate feedbacks would also be subject to high uncertainties.

4.2. Drainage Impact on Annual Carbon Budgets

The bulk of the annual budget differences can be attributed to higher CO_2 emissions at the drained site during the growing season (Kittler et al., 2016). However, as observed with a chamber system (Kwon et al., 2016), more subtle flux shifts also continue further into the non-growing season. The partitioning demonstrates that the restructuring of the ecosystem following sustained drainage (Göckede et al., 2016) leads to higher CO_2 emissions, which are mainly caused by a combination of factors dominated by higher soil temperatures in the upper part of the active layer (Kwon et al., 2016), which in turn result in increasing respiration rates (Lloyd & Taylor, 1994).

Reduced CH_4 emissions are commonly observed under drier and more aerobic conditions (Kim, 2015; Sachs et al., 2008; Sturtevant et al., 2012; Turetsky et al., 2008; Zhang et al., 2012; Zona et al., 2009). The substantial reduction in CH_4 emissions (by approximately 50%) in our study site thus agrees with previous results. Kwon et al. (2017) found that a combination of changes in the soil temperature (i.e., lower temperatures in the anoxic layer and higher temperatures in the oxic layers), microbial communities (reduced abundance of methanogens), and plant communities (reduced abundance of aerenchymatous plant species, which reduced the efficiency of plant-mediated transport) explain changes in CH_4 emission under the influence of a decadal drainage. In an earlier study (Merbold et al., 2009), a significant decrease in CH_4 emission rates immediately following the drainage disturbance was observed, however, using the chamber measurement technique with its inherent uncertainties.

Assuming that similar drainage effects could result from ice-wedge degradation under Arctic warming, our results demonstrate that hydrological disturbance holds the potential to amplify the direct effects of Arctic climate change. Considering integration time frames longer than 100 years, the global warming potential of CH_4 would decrease, thereby leading to a lower relative influence of CH_4 emissions. The combined $CO_{2,\ eq.}$ budgets would be higher than shown in Figure 3. In summary, the $CO_{2,\ eq.}$ budget at the drained site always constitutes a small source for atmospheric carbon. At the control site, where CO_2 uptake dominates over CH_4 emissions for longer time frames, we see a net carbon sink that potentially counteracts climate change effects in the long term.

Positive $CO_{2,\ eq}$. budgets triggered by substantial CH_4 emissions have also been reported by previous studies (Rinne et al., 2007; Wille et al., 2008). However, regarding the net effect of the decadal drainage disturbance, which causes pronounced shifts in exchange fluxes of both CO_2 (Kittler et al., 2016; Kwon et al., 2016) and CH_4 (Kwon et al., 2017), the shifts in the CO_2 budget were found to be the most important. As a result, the $CO_{2,\ eq.}$ budget of the drained ecosystem is positive compared to the control site. This pattern was also reported by Kim (2015). However, the absolute number in this combined budget strongly depends on the integration time frame and the corresponding GWP value for CH_4 (IPCC, 2013). This value, which is linked to the atmospheric lifetime of CH_4, is high for short timescales and continuously declines with increasing length of the integration period. Accordingly, the dominance of the CO_2 signal for the net drainage effect on the $CO_{2,\ eq.}$ budget will even grow when considering time frames of $>$100 years.

This study focused on vertical carbon exchange. However, for a full carbon budget, the lateral transport needs to be taken into consideration (Chapin III et al., 2006). While spring flooding affects both sites similarly, the drainage is expected to be subject to a higher lateral export of carbon because the ditch system installed in 2004 forms a connection to the nearby river. Through this pathway, groundwater can more easily leave the ecosystem and therefore also forms a transportation pathway for dissolved and particulate carbon. Most studies focusing on river systems report a pronounced seasonality in lateral carbon export patterns (Finlay et al., 2006; Holmes et al., 2012; Tank et al., 2012). Differences in carbon enrichment along the stream have also been observed (Crawford et al., 2014). We therefore hypothesize that at the drained site, lateral export through the ditch system constitutes a substantial net carbon loss. This must be taken into account for a full carbon balance assessment. Consequently, consideration of lateral export in the total carbon budget of the drained site can be expected to further increase the net carbon loss found for the vertical exchange processes alone.

4.3. Interannual Variability and Controlling Factors

The year-to-year variability in CO_2 uptake is highly pronounced in the second part of the growing season. In contrast to Parmentier et al. (2011), the highest late growing season uptake is clearly associated with highest mean air temperatures. Because the end of the growing season was defined by the fractional snow cover from MODIS data, the length of the growing season is only indirectly reflected by temperature conditions in the late growing season and can therefore not be used as an indicator at our site. At the same time, prevailing temperature conditions in the first part of the growing season did not significantly affect the CO_2 flux patterns during that time. This finding implies that at our site, carbon cycle processes during the development stage of the vegetation are not limited by temperatures. Instead, the uniform patterns in CO_2 fluxes we observed suggest that once thaw depths have progressed enough to support the growth of vascular plants, a fixed “program,” which is only marginally influenced by environmental conditions, is started. These varied strongly between 2014 and 2016. In contrast, favorable conditions during the late growing season (i.e., higher than normal air temperatures and sufficient water supplies) appear to extend the active vegetation period during which photosynthetic uptake exceeds the respiration losses, thereby leading to significant increases in net growing season CO_2 uptake by the ecosystem. This variation in temperature influence on carbon cycle processes between early and later growing season implies that a bulk growing season averaging can only yield weak causal relationships between environmental conditions and carbon budgets. A subseasonal differentiation can thus significantly improve our capability to identify key drivers of interannual variability.

The patterns in interannual variability of CH_4 budgets are even more complex than those for CO_2 because we observed strongly deviating results between drainage and control sites. Because meteorological forcing is uniform between both treatments, this observation must be caused by the belowground conditions. We assume that drainage has reduced soil water levels so much that the anoxic CH_4 production zone is not subject to upper soil temperature variations (see Table S1 in the supporting information). However, within the control area, shifts in CH_4 emission are closely linked to soil temperatures; higher soil temperatures trigger higher emission rates (Lloyd & Taylor, 1994). As for CO_2, the major part of the interannual variability can be attributed to the second half of the growing season. During that time, we also find different sensitivities to soil temperature conditions between data years. This suggests that the dependence of CH_4 emissions on soil temperatures is further modulated by soil moisture conditions.

5. Conclusion

Our results covering more than 3 years of continuous flux observations within a moist tussock tundra ecosystem demonstrate that under drained conditions, CO_2 uptake and CH_4 emissions are reduced compared to control conditions. Based on the global warming potential metrics under relevant time frames as a net drainage effect, the pronounced reduced sink of CO_2 dominates over reduced CH_4 emissions, thereby implying an increased source of $CO_{2,\ eq.}$ to the atmosphere. This indicates that hydrological disturbances linked to permafrost degradation may amplify the effects of Arctic warming. Year-round measurements highlight the importance of the non-growing season for annual carbon budget assessment. Substantial CH_4 emissions occur particularly during fall, strongly contributing to an overall cold season share of 30% for net annual CH_4 emissions. The cold season emissions account for 60% of CO_2 growing season uptake. The consideration of cold season contributions therefore substantially impacts the annual carbon budgets. The presented findings are also important for the assessment and calibration of land-surface models, which aim to simulate sink/source dynamics of Arctic ecosystems under climate change.

Acknowledgments
This work was supported by the Max-Planck Society, the European Commission (PAGE21 project, FP7-ENV-2011, grant agreement 282700, and PerCCOM project, FP7-PEOPLE-2012-CIG, grant agreement PCIG12-GA-201-333796), the German Ministry of Education and Research (CarboPerm-Project, BMBF grant 03G0836G), the AXA Research Fund (PDOC_2012_W2 campaign, ARF fellowship M. Göckede), and the European Science Foundation (ESF for the activity "Tall Tower and Surface Research Network for Verification of Climate Relevant Emissions of Human Origin", Short Visit Grant, fellowship F. Kittler). The authors appreciate the efforts of NESS staff members, especially Galina Zimova and Nastya Zimova, for organizing field work; they also recognize the team from the Field Experiments and Instrumentation group (MPI-BGC), especially Martin Hertel, for supporting field work. We applied first-last-author-emphasis and equal-contribution (alphabetical sequence) methods for the order of authors (Tscharntke et al., 2007). We thank both anonymous reviewers for their valuable feedback and helpful comments and suggestions that improved our manuscript. Data are available from the European Fluxes Database Cluster (http://www.europe-fluxdata.eu/home) with site-code "RU-Che" for the control site and "RU-Ch2" for the drained site.

References

Arneth, A., Kurbatova, J., Kolle, O., Shibistova, O. B., Lloyd, J., Vygodskaya, N. N., & Schulze, E. D. (2002). Comparative ecosystem-atmosphere exchange of energy and mass in a European Russian and a central Siberian bog II. Interseasonal and interannual variability of CO_2 fluxes. *Tellus B*, *54*(5), 514–530. https://doi.org/10.1034/j.1600-0889.2002.01349.x

Aurela, M., Laurila, T., & Tuovinen, J.-P. (2004). The timing of snow melt controls the annual CO_2 balance in a subarctic fen. *Geophysical Research Letters*, *31*, L16119. https://doi.org/10.1029/2004GL020315

Aurela, M., Riutta, T., Laurila, T., Tuovinen, J.-P., Vesala, T., Tuittila, E. S., … Laine, J. (2007). CO_2 exchange of a sedge fen in southern Finland—The impact of a drought period. *Tellus B*, *59*(5), 826–837. https://doi.org/10.1111/j.1600-0889.2007.00309.x

Belshe, E. F., Schuur, E. A. G., & Bolker, B. M. (2013). Tundra ecosystems observed to be CO_2 sources due to differential amplification of the carbon cycle. *Ecology Letters*, *16*(10), 1307–1315. https://doi.org/10.1111/ele.12164

Burba, G. G., Anderson, D. J., Xu, L., & McDermitt, D. K. (2006). Correcting apparent off-season CO_2 uptake due to surface heating of a an open path gas analyzer: Process report of an ongoing study. In *Proceedings of 27th Annual Conference on Agricultural and Forest meteorology* (p. 13). San Diego, CA.

Chapin, F. S. III, Woodwell, G. M., Randerson, J. T., Rastetter, E. B., Lovett, G. M., Baldocchi, D. D., … Schulze, E. D. (2006). Reconciling carbon-cycle concepts, terminology, and methods. *Ecosystems*, *9*(7), 1041–1050. https://doi.org/10.1007/s10021-005-0105-7

Christensen, T. R. (2014). Climate science: Understand Arctic methane variability. *Nature*, *509*(7500), 279–281. https://doi.org/10.1038/509279a

Christiansen, C. T., Schmidt, N. M., & Michelsen, A. (2012). High Arctic dry heath CO_2 exchange during the early cold season. *Ecosystems*, *15*(7), 1083–1092. https://doi.org/10.1007/s10021-012-9569-4

Corradi, C., Kolle, O., Walter, K., Zimov, S. A., & Schulze, E. D. (2005). Carbon dioxide and methane exchange of a north-east Siberian tussock tundra. *Global Change Biology*, *11*(11), 1910–1925. https://doi.org/10.1111/j.1365-2486.2005.01023.x

Crawford, J. T., Lottig, N. R., Stanley, E. H., Walker, J. F., Hanson, P. C., Finlay, J. C., & Striegl, R. G. (2014). CO_2 and CH_4 emissions from streams in a lake-rich landscape: Patterns, controls, and regional significance. *Global Biogeochemical Cycles*, *28*, 197–210. https://doi.org/10.1002/2013GB004661

Emmerton, C. A., Louis, V. L. S., Lehnherr, I., Humphreys, E. R., Rydz, E., & Kosolofski, H. R. (2014). The net exchange of methane with high Arctic landscapes during the summer growing season. *Biogeosciences*, *11*(12), 3095–3106. https://doi.org/10.5194/bg-11-3095-2014

Euskirchen, E. S., Bret-Harte, M. S., Scott, G. J., Edgar, C., & Shaver, G. R. (2012). Seasonal patterns of carbon dioxide and water fluxes in three representative tundra ecosystems in northern Alaska. *Ecosphere*, *3*(1), 1–19. https://doi.org/10.1890/ES11-00202.1

Euskirchen, E. S., Bret-Harte, M. S., Shaver, G. R., Edgar, C. W., & Romanovsky, V. E. (2016). Long-term release of carbon dioxide from Arctic tundra ecosystems in Alaska. *Ecosystems*, *20*(5), 960–974. https://doi.org/10.1007/s10021-016-0085-9

Finlay, J., Neff, J., Zimov, S., Davydova, A., & Davydov, S. (2006). Snowmelt dominance of dissolved organic carbon in high-latitude watersheds: Implications for characterization and flux of river DOC. *Geophysical Research Letters*, *33*, L10401. https://doi.org/10.1029/2006GL025754

Foken, T., & Wichura, B. (1996). Tools for quality assessment of surface-based flux measurements. *Agricultural and Forest Meteorology*, *78*(1-2), 83–105. https://doi.org/10.1016/0168-1923(95)02248-1

Foken, T., Göockede, M., Mauder, M., Mahrt, L., Amiro, B., & Munger, W. (2005). Post-field data quality control. In X. Lee, W. Massman, & B. Law (Eds.), *Handbook of micrometeorology: A guide for surface flux measurement and analysis* (pp. 181–208). Dordrecht, Netherlands: Springer. https://doi.org/10.1007/1-4020-2265-4_9

Foken, T., Leuning, R., Oncley, S. P., Mauder, M., & Aubinet, M. (2012). Corrections and data quality. In M. Aubinet, T. Vesala, & D. Papale (Eds.), *Eddy covariance—A practical guide to measurement and data analysis* (pp. 85–131). Berlin: Springer.

Fratini, G., & Mauder, M. (2014). Towards a consistent eddy-covariance processing: An intercomparison of EddyPro and TK3. *Atmospheric Measurement Techniques*, *7*(7), 2273–2281. https://doi.org/10.5194/amt-7-2273-2014

Göckede, M., Kittler, F., Kwon, M. J., Burjack, I., Heimann, M., Kolle, O., … Zimov, S. (2016). Shifts in permafrost ecosystem structure following a decade-long drainage increase energy transfer to the atmosphere, but reduce thaw depth. *The Cryosphere Discussions*, *2016*, 1–38. https://doi.org/10.5194/tc-2016-212

Goodrich, J. P., Oechel, W. C., Gioli, B., Moreaux, V., Murphy, P. C., Burba, G., & Zona, D. (2016). Impact of different eddy covariance sensors, site set-up, and maintenance on the annual balance of CO_2 and CH_4 in the harsh Arctic environment. *Agricultural and Forest Meteorology*, *228-229*, 239–251. https://doi.org/10.1016/j.agrformet.2016.07.008

Holmes, R. M., McClelland, J. W., Peterson, B. J., Tank, S. E., Bulygina, E., Eglinton, T. I., … Zimov, S. A. (2012). Seasonal and annual fluxes of nutrients and organic matter from large rivers to the Arctic Ocean and surrounding seas. *Estuaries and Coasts*, *35*(2), 369–382. https://doi.org/10.1007/s12237-011-9386-6

Hugelius, G., Strauss, J., Zubrzycki, S., Harden, J. W., Schuur, E. A. G., Ping, C. L., … Kuhry, P. (2014). Estimated stocks of circumpolar permafrost carbon with quantified uncertainty ranges and identified data gaps. *Biogeosciences*, *11*(23), 6573–6593. https://doi.org/10.5194/bg-11-6573-2014

IPCC (2013). Climate change 2013: The physical science basis. Contribution of working group I to the fifth assessment report of the Intergovernmental Panel on Climate Change (1535 pp.). Cambridge, United Kingdom and New York, NY: Cambridge University Press. https://doi.org/10.1017/CBO9781107415324

Jammet, M., Dengel, S., Kettner, E., Parmentier, F. J. W., Wik, M., Crill, P., & Friborg, T. (2017). Year-round CH_4 and CO_2 flux dynamics in two contrasting freshwater ecosystems of the subarctic. *Biogeosciences Discussions*, *2017*, 1–49. https://doi.org/10.5194/bg-2016-466

Järvi, L., Mammarella, I., Eugster, W., Ibrom, A., Siivola, E., Dellwik, E., … Vesala, T. (2009). Comparison of net CO_2 fluxes measured with open- and closed-path infrared gas analyzers in an urban complex environment. *Boreal Environment Research*, *14*(4), 499–514.

Jorgenson, M. T., Shur, Y. L., & Pullman, E. R. (2006). Abrupt increase in permafrost degradation in Arctic Alaska. *Geophysical Research Letters*, *33*, L02503. https://doi.org/10.1029/2005GL024960

Kaufman, D. S., Schneider, D. P., McKay, N. P., Ammann, C. M., Bradley, R. S., Briffa, K. R., … Thomas, E. (2009). Recent warming reverses long-term arctic cooling. *Science*, *325*(5945), 1236–1239. https://doi.org/10.1126/science.1173983

Kim, Y. (2015). Effect of thaw depth on fluxes of CO_2 and CH_4 in manipulated Arctic coastal tundra of Barrow, Alaska. *The Science of the Total Environment*, *505*, 385–389. https://doi.org/10.1016/j.scitotenv.2014.09.046

Kirschbaum, M. U. F. (1995). The temperature-dependence of soil organic-matter decomposition, and the effect of global warming on soil organic-C storage. *Soil Biology and Biochemistry*, *27*(6), 753–760. https://doi.org/10.1016/0038-0717(94)00242-S

Kittler, F., Burjack, I., Corradi, C. A. R., Heimann, M., Kolle, O., Merbold, L., … Göckede, M. (2016). Impacts of a decadal drainage disturbance on surface–atmosphere fluxes of carbon dioxide in a permafrost ecosystem. *Biogeosciences*, *13*(18), 5315–5332. https://doi.org/10.5194/bg-13-5315-2016

Kittler, F., Eugster, W., Foken, T., Heimann, M., Kolle, O., & Gockede, M. (2017). High-quality eddy-covariance CO_2 budgets under cold climate conditions. *Journal of Geophysical Research: Biogeosciences*, *122*, 2064–2084. https://doi.org/10.1002/2017JG003830

Kolle, O., & Rebmann, C. (2007). EddySoft; documentation of a software package to acquire and process eddy covariance Data*Rep*., Jena.

Kutzbach, L., Wille, C., & Pfeiffer, E. M. (2007). The exchange of carbon dioxide between wet arctic tundra and the atmosphere at the Lena River Delta, northern Siberia. *Biogeosciences*, *4*(5), 869–890. https://doi.org/10.5194/bg-4-869-2007

Kwon, M. J., Heimann, M., Kolle, O., Luus, K. A., Schuur, E. A. G., Zimov, N., … Göckede, M. (2016). Drainage reduces CO_2 uptake and increases CO_2 efflux by a Siberian floodplain due to shifts in vegetation community and soil thermal characteristics. *Biogeosciences*, *13*(14), 4219–4235. https://doi.org/10.5194/bg-13-4219-2016

Kwon, M. J., Beulig, F., Ilie, I., Wildner, M., Küsel, K., Merbold, L., … Göckede, M. (2017). Plants, microorganisms, and soil temperatures contribute to a decrease in methane fluxes on a drained Arctic floodplain. *Global Change Biology*, *23*(6), 2396–2412. https://doi.org/10.1111/gcb.13558

Laurila, T., Soegaard, H., Lloyd, C. R., Aurela, M., Tuovinen, J. P., & Nordstroem, C. (2001). Seasonal variations of net CO_2 exchange in European Arctic ecosystems. *Theoretical and Applied Climatology*, *70*(1-4), 183–201. https://doi.org/10.1007/s007040170014

Liljedahl, A. K., Boike, J., Daanen, R. P., Fedorov, A. N., Frost, G. V., Grosse, G., … Zona, D. (2016). Pan-Arctic ice-wedge degradation in warming permafrost and its influence on tundra hydrology. *Nature Geoscience*, *9*(4), 312–318. https://doi.org/10.1038/ngeo2674

Liu, H. P., Peters, G., & Foken, T. (2001). New equations for sonic temperature variance and buoyancy heat flux with an omnidirectional sonic anemometer. *Boundary-Layer Meteorology*, *100*(3), 459–468. https://doi.org/10.1023/A:1019207031397

Lloyd, J., & Taylor, J. A. (1994). On the temperature-dependence of soil respiration. *Functional Ecology*, *8*(3), 315–323. https://doi.org/10.2307/2389824

Lüers, J., Westermann, S., Piel, K., & Boike, J. (2014). Annual CO_2 budget and seasonal CO_2 exchange signals at a high Arctic permafrost site on Spitsbergen, Svalbard archipelago. *Biogeosciences*, *11*(22), 6307–6322. https://doi.org/10.5194/bg-11-6307-2014

Lund, M., Falk, J. M., Friborg, T., Mbufong, H. N., Sigsgaard, C., Soegaard, H., & Tamstorf, M. P. (2012). Trends in CO_2 exchange in a high Arctic tundra heath, 2000–2010. *Journal of Geophysical Research*, *117*, G02001. https://doi.org/10.1029/2011JG001901

Mastepanov, M., Sigsgaard, C., Dlugokencky, E. J., Houweling, S., Strom, L., Tamstorf, M. P., & Christensen, T. R. (2008). Large tundra methane burst during onset of freezing. *Nature*, *456*(7222), 628–630. https://doi.org/10.1038/nature07464

Mastepanov, M., Sigsgaard, C., Tagesson, T., Ström, L., Tamstorf, M. P., Lund, M., & Christensen, T. R. (2013). Revisiting factors controlling methane emissions from high-Arctic tundra. *Biogeosciences*, *10*(7), 5139–5158. https://doi.org/10.5194/bg-10-5139-2013

Mauder, M., & Foken, T. (2015). Eddy-covariance software TK3. https://doi.org/10.5281/zenodo.20349

McGuire, A. D., Anderson, L. G., Christensen, T. R., Dallimore, S., Guo, L. D., Hayes, D. J., … Roulet, N. (2009). Sensitivity of the carbon cycle in the Arctic to climate change. *Ecological Monographs*, *79*(4), 523–555. https://doi.org/10.1890/08-2025.1

McGuire, A. D., Christensen, T. R., Hayes, D., Heroult, A., Euskirchen, E., Kimball, J. S., … Yi, Y. (2012). An assessment of the carbon balance of Arctic tundra: Comparisons among observations, process models, and atmospheric inversions. *Biogeosciences*, *9*(8), 3185–3204. https://doi.org/10.5194/bg-9-3185-2012

Merbold, L., Kutsch, W. L., Corradi, C., Kolle, O., Rebmann, C., Stoy, P. C., … Schulze, E. D. (2009). Artificial drainage and associated carbon fluxes (CO_2/CH_4) in a tundra ecosystem. *Global Change Biology*, *15*(11), 2599–2614. https://doi.org/10.1111/j.1365-2486.2009.01962.x

Mikhailov, O. A., Zagirova, S. V., Miglovets, M. N., & Wille, C. (2013). Carbon dioxide fluxes in the ecosystem of meso-oligotrophic peatland during the transition period from autumn to winter. *Contemporary Problems of Ecology*, *6*(2), 143–148. https://doi.org/10.1134/S1995425513020108

Moore, C. J. (1986). Frequency response corrections for eddy correlation systems. *Boundary-Layer Meteorology*, *37*(1-2), 17–35. https://doi.org/10.1007/Bf00122754

Moore, T. R., De Young, A., Bubier, J. L., Humphreys, E. R., Lafleur, P. M., & Roulet, N. T. (2011). A multi-year record of methane flux at the Mer Bleue Bog, Southern Canada. *Ecosystems*, *14*(4), 646–657. https://doi.org/10.1007/s10021-011-9435-9

Morgner, E., Elberling, B., Strebel, D., & Cooper, E. J. (2010). The importance of winter in annual ecosystem respiration in the High Arctic: Effects of snow depth in two vegetation types. *Polar Research*, *29*(1), 58–74. https://doi.org/10.1111/j.1751-8369.2010.00151.x

Oechel, W. C., Vourlitis, G., & Hastings, S. J. (1997). Cold season CO_2 emission from Arctic soils. *Global Biogeochemical Cycles*, *11*(2), 163–172. https://doi.org/10.1029/96GB03035

Oechel, W. C., Vourlitis, G. L., Hastings, S. J., Ault, R. P., & Bryant, P. (1998). The effects of water table manipulation and elevated temperature on the net CO_2 flux of wet sedge tundra ecosystems. *Global Change Biology*, *4*(1), 77–90. https://doi.org/10.1046/j.1365-2486.1998.00110.x

Oechel, W. C., Laskowski, C. A., Burba, G., Gioli, B., & Kalhori, A. A. M. (2014). Annual patterns and budget of CO_2 flux in an Arctic tussock tundra ecosystem. *Journal of Geophysical Research: Biogeosciences*, *119*, 323–339. https://doi.org/10.1002/2013JG002431

Overland, J. E., Wang, M., Walsh, J. E., & Stroeve, J. C. (2014). Future Arctic climate changes: Adaptation and mitigation time scales. *Earth's Future*, *2*(2), 68–74. https://doi.org/10.1002/2013EF000162

Parmentier, F. J. W., van der Molen, M. K., van Huissteden, J., Karsanaev, S. A., Kononov, A. V., Suzdalov, D. A., … Dolman, A. J. (2011). Longer growing seasons do not increase net carbon uptake in the northeastern Siberian tundra. *Journal of Geophysical Research*, *116*, G04013. https://doi.org/10.1029/2011JG001653

Philipp, R. S., Mark, A. K. G., Sabine, B. R., Nanna, B., Bo, E., & Elisabeth, J. C. (2016). High Arctic plant phenology is determined by snowmelt patterns but duration of phenological periods is fixed: An example of periodicity. *Environmental Research Letters*, *11*(12), 125006.

Pirk, N., Sievers, J., Mertes, J., Parmentier, F. J. W., Mastepanov, M., & Christensen, T. R. (2017). Spatial variability of CO2 uptake in polygonal tundra: Assessing low-frequency disturbances in eddy covariance flux estimates. *Biogeosciences*, *14*(12), 3157–3169. https://doi.org/10.5194/bg-14-3157-2017

Reichstein, M., Falge, E., Baldocchi, D., Papale, D., Aubinet, M., Berbigier, P., … Valentini, R. (2005). On the separation of net ecosystem exchange into assimilation and ecosystem respiration: Review and improved algorithm. *Global Change Biology*, *11*(9), 1424–1439. https://doi.org/10.1111/j.1365-2486.2005.001002.x

Rinne, J., Riutta, T., Pihlatie, M., Aurela, M., Haapanala, S., Tuovinen, J.-P., … Vesala, T. (2007). Annual cycle of methane emission from a boreal fen measured by the eddy covariance technique. *Tellus B*, *59*(3), 449–457. https://doi.org/10.1111/j.1600-0889.2007.00261.x

Runkle, B. R. K., Sachs, T., Wille, C., Pfeiffer, E. M., & Kutzbach, L. (2013). Bulk partitioning the growing season net ecosystem exchange of CO_2 in Siberian tundra reveals the seasonality of its carbon sequestration strength. *Biogeosciences*, *10*(3), 1337–1349. https://doi.org/10.5194/bg-10-1337-2013

Sachs, T., Wille, C., Boike, J., & Kutzbach, L. (2008). Environmental controls on ecosystem-scale CH_4 emission from polygonal tundra in the Lena River Delta, Siberia. *Biogeosciences*, *113*, G00A03. https://doi.org/10.1029/2007JG000505

Schuur, E. A. G., McGuire, A. D., Schädel, C., Grosse, G., Harden, J. W., Hayes, D. J., … Vonk, J. E. (2015). Climate change and the permafrost carbon feedback. *Nature*, *520*(7546), 171–179. https://doi.org/10.1038/nature14338

Serreze, M. C., Walsh, J. E., Chapin, F. S. III, Osterkamp, T., Dyurgerov, M., Romanovsky, V., … Barry, R. G. (2000). Observational evidence of recent change in the northern high-latitude environment. *Climatic Change*, *46*(1/2), 159–207. https://doi.org/10.1023/A:1005504031923

Serreze, M. C., Barrett, A. P., Stroeve, J. C., Kindig, D. N., & Holland, M. M. (2009). The emergence of surface-based Arctic amplification. *The Cryosphere*, *3*(1), 11–19. https://doi.org/10.5194/tc-3-11-2009

Strack, M., Kellner, E., & Waddington, J. M. (2006). Effect of entrapped gas on peatland surface level fluctuations. *Hydrological Processes*, *20*(17), 3611–3622. https://doi.org/10.1002/Hyp.6518

Sturtevant, C. S., Oechel, W. C., Zona, D., Kim, Y., & Emerson, C. E. (2012). Soil moisture control over autumn season methane flux, Arctic Coastal Plain of Alaska. *Biogeosciences*, *9*(4), 1423–1440. https://doi.org/10.5194/bg-9-1423-2012

Tagesson, T., Mölder, M., Mastepanov, M., Sigsgaard, C., Tamstorf, M. P., Lund, M., … Ström, L. (2012). Land-atmosphere exchange of methane from soil thawing to soil freezing in a high-Arctic wet tundra ecosystem. *Global Change Biology*, *18*(6), 1928–1940. https://doi.org/10.1111/j.1365-2486.2012.02647.x

Tank, S. E., Raymond, P. A., Striegl, R. G., McClelland, J. W., Holmes, R. M., Fiske, G. J., & Peterson, B. J. (2012). A land-to-ocean perspective on the magnitude, source and implication of DIC flux from major Arctic rivers to the Arctic Ocean. *Global Biogeochemical Cycles*, *26*, GB4018. https://doi.org/10.1029/2011GB004192

Tscharntke, T., Hochberg, M. E., Rand, T. A., Resh, V. H., & Krauss, J. (2007). Author sequence and credit for contributions in multiauthored publications. *PLoS Biology*, *5*(1), e18–e14. https://doi.org/10.1371/journal.pbio.0050018

Turetsky, M. R., Treat, C. C., Waldrop, M. P., Waddington, J. M., Harden, J. W., & McGuire, A. D. (2008). Short-term response of methane fluxes and methanogen activity to water table and soil warming manipulations in an Alaskan peatland. *Journal of Geophysical Research*, *113*, G00A10. https://doi.org/10.1029/2007JG000496

Turetsky, M. R., Kotowska, A., Bubier, J., Dise, N. B., Crill, P., Hornibrook, E. R. C., … Wilmking, M. (2014). A synthesis of methane emissions from 71 northern, temperate, and subtropical wetlands. *Global Change Biology*, *20*(7), 2183–2197. https://doi.org/10.1111/gcb.12580

Webb, E. K., Pearman, G. I., & Leuning, R. (1980). Correction of flux measurements for density effects due to heat and water vapour transfer. *Quarterly Journal of the Royal Meteorological Society*, *106*(447), 85–100. https://doi.org/10.1002/qj.49710644707

Webb, E. E., Schuur, E. A. G., Natali, S. M., Oken, K. L., Bracho, R., Krapek, J. P., … Nickerson, N. R. (2016). Increased wintertime CO_2 loss as a result of sustained tundra warming. *Journal of Geophysical Research: Biogeosciences*, *121*, 249–265. https://doi.org/10.1002/2014JG002795

Wille, C., Kutzbach, L., Sachs, T., Wagner, D., & Pfeiffer, E. M. (2008). Methane emission from Siberian arctic polygonal tundra: Eddy covariance measurements and modeling. *Global Change Biology*, *14*(6), 1395–1408. https://doi.org/10.1111/j.1365-2486.2008.01586.x

10.1002/2017GB005774

Yu, Z., Wang, J., Liu, S., Piao, S., Ciais, P., Running, S. W., … Sun, P. (2016). Decrease in winter respiration explains 25% of the annual northern forest carbon sink enhancement over the last 30 years. *Global Ecology and Biogeography*, *25*(5), 586–595. https://doi.org/10.1111/geb.12441

Zhang, Y., Sachs, T., Li, C., & Boike, J. (2012). Upscaling methane fluxes from closed chambers to eddy covariance based on a permafrost biogeochemistry integrated model. *Global Change Biology*, *18*(4), 1428–1440. https://doi.org/10.1111/j.1365-2486.2011.02587.x

Zimov, S. A., Davidov, S. P., Voropaev, Y. V., Prosiannikov, S. F., Semiletov, I. P., Chapin, M. C., & Chapin, F. S. III (1996). Siberian CO_2 efflux in winter as a CO_2 source and cause of seasonality in atmospheric CO_2. *Climatic Change*, *33*(1), 111–120. https://doi.org/10.1007/Bf00140516

Zona, D., Oechel, W. C., Kochendorfer, J., Paw U, K. T., Salyuk, A. N., Olivas, P. C., … Lipson, D. A. (2009). Methane fluxes during the initiation of a large-scale water table manipulation experiment in the Alaskan Arctic tundra. *Global Biogeochemical Cycles*, *23*, Gb2013. https://doi.org/10.1029/2009GB003487

Zona, D., Lipson, D. A., Paw, K. T., Oberbauer, S. F., Olivas, P., Gioli, B., & Oechel, W. C. (2012). Increased CO_2 loss from vegetated drained lake tundra ecosystems due to flooding. *Global Biogeochemical Cycles*, *26*, Gb2004. https://doi.org/10.1029/2011GB004037

Zona, D., Gioli, B., Commane, R., Lindaas, J., Wofsy, S. C., Miller, C. E., … Oechel, W. C. (2016). Cold season emissions dominate the Arctic tundra methane budget. *Proceedings of the National Academy of Sciences of the United States of America*, *113*(1), 40–45. https://doi.org/10.1073/pnas.1516017113